ARTICLES

Examination of DFT and TDDFT Methods I

Yi-Gui Wang*

Department of Chemistry, Yale University, New Haven, Connecticut 06520-8107

Received: April 30, 2009; Revised Manuscript Received: July 12, 2009

We investigated DFT and TDDFT methods in the sense of the molecular orbital (MO) theory and in the framework of the quantum theory of atoms in molecules (QT-AIM). The detailed investigations for the ground state and the $\pi \rightarrow \pi^*$ excited state of ethene clarified three aspects about DFT and TDDFT methods: First, the DFT methods included electron correlation effects by directly changing MO energies and MO electron density distributions. Second, MO occupation numbers explained why the delocalization indices (DIs) obtained from DFT wave function files apparently differed from DIs obtained from the conventional correlated wave function files. At last, the significant underestimation of the excitation energy for the $\pi \rightarrow \pi^*$ adiabatic excited states of ethene by TDDFT methods can be attributed to the exact degeneracy of HOMO (π) and LUMO (π^*), a special case of charge transfer (CT) excited states.

1. Introduction

Density analysis is independent of the density functional theory (DFT), although both are based on electron density in principle. The DFT methods are based on the Kohn−Hohenberg theory, for which the properties are uniquely related to the electron density,[1−10] whereas the density used in density analysis can be obtained from experiments or from calculations.[11] To do density analyses, the gradient of energy for a specific method is needed to write out wave function files. The electron pair density (delocalization indices (DIs)) can be analyzed by eq 1[12−14]

$$\delta(A,B) = 2\sum_{l,m} n_l^{1/2} n_m^{1/2} S_{lm}(\Omega) S_{lm}(\Omega') \qquad (1)$$

Equation 1 was identical to Fulton's sharing index, which was obtained by integrating the exchange-correlation second-order density and therefore was an approximation to the true DI.[15] Because a molecular orbital (MO) usually extends over the whole molecule in the MO theory, the quantum theory of atoms in molecules (QT-AIM) was necessary to separate the molecule into atomic basins (Ω) on the basis of the topology of electronic density. Every MO interacts with other MOs, and the interactions were associated with separated atomic basins and expressed by the elements $S_{lm}(\Omega)$ of atomic overlap matrix (AOM). The symbols n_l and n_m stand for MO occupation numbers, and Ω and Ω' represent different basins.

The DI was formally developed as the electron pair density,[12] and only at the HF level could the equation of electron pair density be simplified into an equation similar to eq 1, in which $n_l = n_m = 2$.[13] The exact pair density including correlation effects was worked out and developed at the CISD level.[13,14] We and others found that the simple eq 1 was applicable to conventional correlated methods and DFT methods, provided that the wave function files were written out as the expression of natural MOs.[16a,b,17] We further extended the application of eq 1 to study the excited states at both CIS and EOM-CCSD levels.[16c] As far as DFT methods are concerned, it was peculiar that for the ground-state DFT, DIs of multiple bonds were close to HF DIs, whereas the DIs of conventional correlation methods were significantly reduced.[10,13,18] Because the correlation effects were included in DFT methods by definition, one interesting question may be asked: How can we interpret the apparent discrepancy in DIs?

For the excited states, the gradient of energy was worked out by Van Caillie and Amos at the TD-LDA level to optimize excited-state structures almost 10 years ago,[19] and this technique is now available for all new functionals in Gaussian program packages.[20] In this article, we investigated the ground state and the $\tilde{A}\ ^1B_{1u}(\pi \rightarrow \pi^*)$ excited state of ethene with a total of 25 DFT (TDDFT) functionals. A detailed comparison was made between the DFT results and the results from the other two families of methods: HF (CIS) and CCSD (EOM-CCSD). A detailed analysis was also carried out to explain why the B3LYP DIs were different from CCSD DIs but similar to HF DIs.

2. $\tilde{A}\ ^1B_{1u}(\pi \rightarrow \pi^*)$ Excited State of Ethene

2.1. Optimization. Ethene is a prototype compound consisting of one C=C double bond and has naturally been the ideal subject of both extensive experimental and theoretical studies. For the valence $\pi \rightarrow \pi^*$ adiabatic excited state of ethene, the VUV experiment indicated an uncertain dihedral angle of 37−90° and a C−C bond length of ∼1.4 Å.[21] A recent MR-CISD study concluded that the D_{2d} structure (C−C is 1.386 Å) was actually a saddle point upon pyramidalization of one methylene group,[22a] and another multireference calculation indicated that the C−C distance for the twisted $\pi \rightarrow \pi^*$ excited state (D_{2d}) is 1.369 Å.[22b] Therefore, the true C−C bond length seems to be ∼1.38 Å, and the $\pi \rightarrow \pi^*$ state possesses multiple-configuration character.[23,24] In the early 1990s, the simple single-reference method CIS was found to predict reasonable adiabatic

* Corresponding author.

10.1021/jp904007j CCC: $40.75
Published on Web 09/16/2009

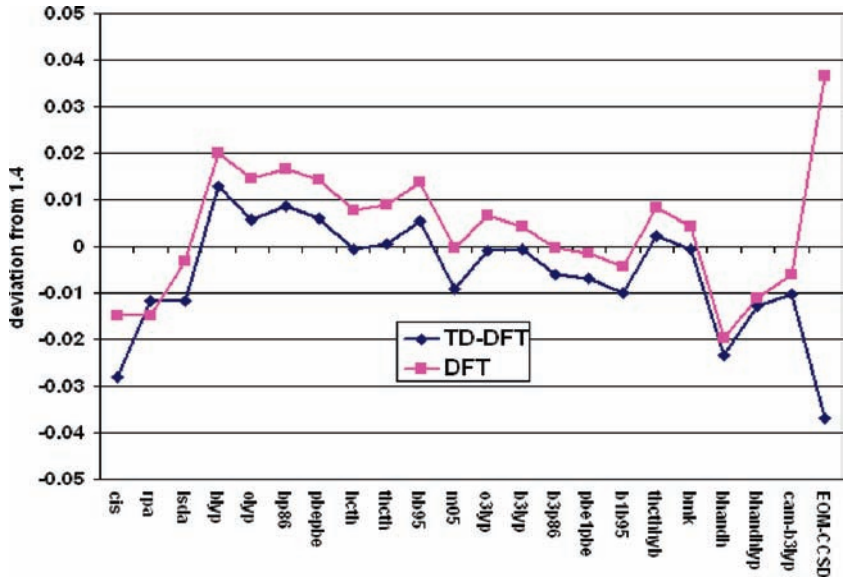

Figure 1. Deviations of the C−C bond from 1.40 Å. The H−C−C−H dihedral angle was kept at 87.2°. The blue line indicates adiabatic excited states (TDDFT), and the pink line indicates twisted ground states (DFT).

$\pi \rightarrow \pi^*$ excited-state structures; the bond length and dihedral angle were 1.3742 Å and 88.47° at the CIS/6-311+G* level, respectively.[25] We later optimized the $\pi \rightarrow \pi^*$ excited state at the EOM-CCSD/6-311++G** level. The optimized HCCH dihedral angle was 87.2°, and the optimized C−C bond length was 1.344 Å.[26]

With the implementation of TDDFT energy gradients,[20] we optimized the adiabatic excited-state structures. Unfortunately, none of the functionals could give a converged structure for the $\pi \rightarrow \pi^*$ adiabatic excited state of ethene, so we optimized only the C−C bond length while restraining all other parameters to be EOM-CCSD-optimized parameters (dihedral angle was 87.2°, C−H bonds were 1.09 Å, and ∠HCC was 123.9°). The optimizations were also carried out for the twisted ground states (Figure 1 and Table S1a in the Supporting Information with both 6-311++G** and aug-cc-pVTZ basis sets). For the adiabatic excited states, all TDDFT methods predicted longer C−C bond lengths than both CIS and EOM-CCSD methods. In contrast, all DFT methods regarding the 87° twisted ground state produced C−C bond lengths of ∼1.4 Å, falling between the results of HF and CCSD. All TDDFT methods seem to be flexible in handling the twisted $\pi \rightarrow \pi^*$ excited state. Some studies indicated that DFT methods were able to treat diradical species.[27] As a rule, for both adiabatic excited states and twisted ground states, pure functionals (shown toward left of Figure 1) predict longer C−C bond lengths than hybrid functionals (shown toward the right) do. The DFT methods predict slightly shorter C−C bond lengths (by 0.002−0.005 Å) by aug-cc-PVTZ basis sets than by 6-311++G** (Table S1a in the Supporting Information).

2.2. Excitation Energies: Implications of HOMO and LUMO. Ethene has a planar structure in its ground state and a twisted structure in its $\pi \rightarrow \pi^*$ adiabatic excited state. The CCSD-optimized structure (ground state) and the EOM-CCSD-optimized structure (excited state) were used in the following discussion. Besides the usual vertical excitation energy and adiabatic excitation energy, we additionally separated the adiabatic excitation energy into two components: the distortion energy (the energy needed to convert a planar structure into a twisted structure) and the subsequent energy needed to excite electrons from the distorted structure. The latter was sometimes called vertical de-excitation energy because of its connection to fluorescence in some systems.[28] We will not adopt this designation to avoid confusion in our following discussions. In Figure 2, the vertical excitation energies were subtracted by 8.0 eV to maintain the same scale as the other lines; also, all other energies are subtracted by the corresponding CCSD or EOM-CCSD values.

The value of 8.0 eV (7.9 ± 0.1 eV) was estimated to be the true vertical excitation energy by Lindh and Roos.[23] EOM-CCSD/6-311++G** predicted a reasonable vertical excitation energy of 8.17 eV (only 0.17 eV higher), whereas TDDFT vertical excitation energies were too low (by ∼0.5 eV). The adiabatic excitation energy was 5.98 eV at EOM-CCSD/6-311++G** level, which was in reasonable agreement with the experimental value of 5.50 eV. All TDDFT methods predicted significantly lower adiabatic excitation energies than the EOM-CCSD method (by ∼1.5 eV). In comparison with CCSD (EOM-CCSD) results, DFT methods overestimated distortion energy by a relatively small amount (0.1 to 0.3 eV), whereas TDDFT methods significantly underestimated the excitation energy from the twisted structure (red line in Figure 2, by 1.5 to 1.8 eV). The significant underestimation of adiabatic excitation energies by TDDFT methods came from the latter (Figure 2). The TDDFT methods introduced only negligible changes in excitation energies by aug-cc-pVTZ basis sets in comparison with 6-311++G** basis sets (Table S1b in the Supporting Information).

Why do TDDFT methods predict substantially low excitation energies for both vertical and adiabatic excited states? We can find clues from the energies of MOs. The HOMO−LUMO excitation was the major component of the $\pi \rightarrow \pi^*$ excited states. Figure 3 plots energies (cf. Table S1c in the Supporting Information for exact energies with both 6-311++G** and aug-cc-pVTZ basis sets) for a few MOs for both planar and twisted ground states. For all DFT functionals, Kohn−Sham HOMO energies were generally higher and Kohn−Sham LUMO energies were consistently lower than those of the HF approach. As a result, HOMO−LUMO gaps were typically smaller than the HF gaps, so the excitation energies were substantially low. Because of the mixing of HF in hybrid functionals, the hybrid DFT methods had enlarged HOMO−LUMO gaps and, in general, increased excitation energies. For the twisted ground state, the gap between HOMO and LUMO reduced so signifi-

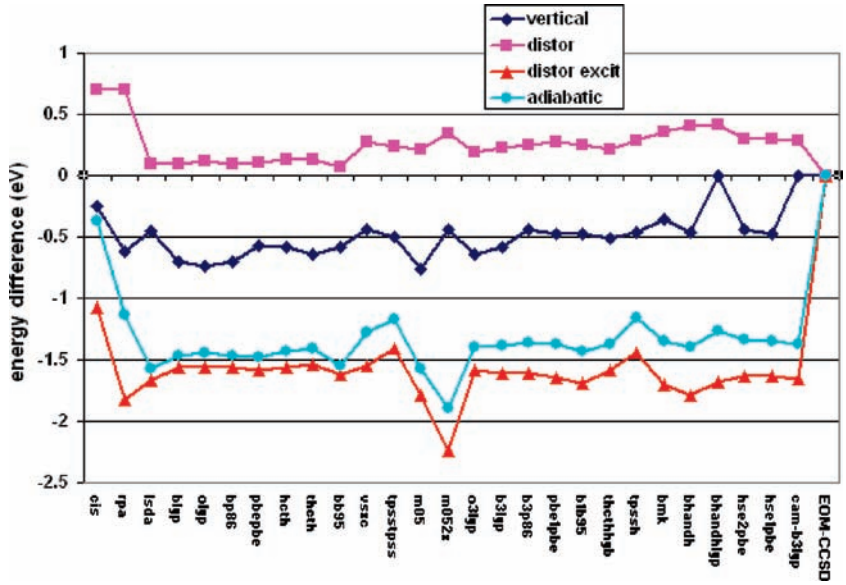

Figure 2. Excitation energies for ethene. (The vertical excitation energies are subtracted by 8.0 eV. All other energies are subtracted by CCSD or EOM-CCSD values. The methods are (from left to right): cis, rpa, lsda, blyp, olyp, bp86, pbepbe, hcth, thcth, bb95, vsxc, tpsstpss, m05, m052x, o3lyp, b3lyp, b3p86, pbe1pbe, b1b95, thcthhyb, tpssh, bmk, bhandh, bhandhlyp, hse2pbe, hse1pbe, cam-b3lyp, EOM-CCSD).

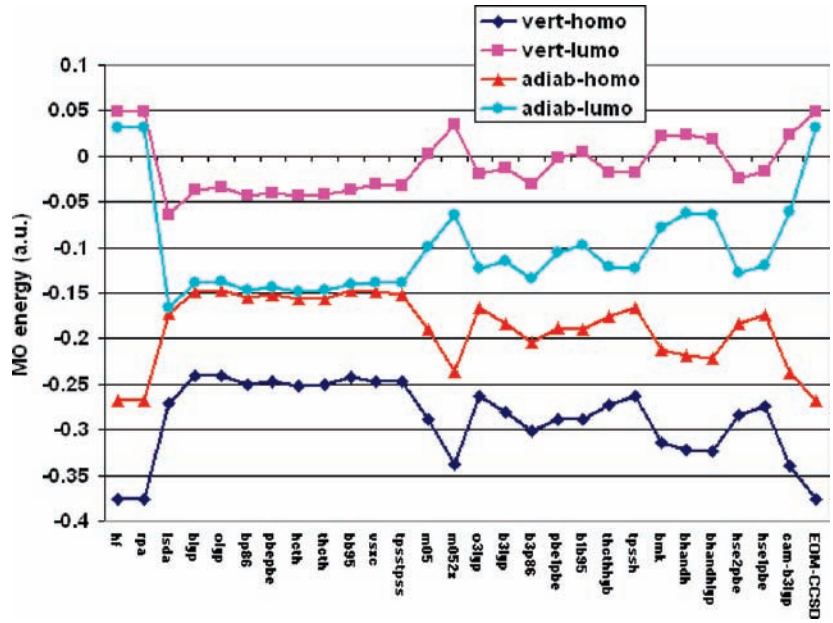

Figure 3. Energy of FMOs (methods are the same as those of Figure 2).

cantly that two MOs were almost degenerate, which was especially evident for pure functionals. The relationship between the HOMO−LUMO gap and the excitation energy should not be over emphasized because the total energy is not simply the sum of all individual MO energies (which is only true in the case of single-electron Hückel theory). Nonetheless, there is no doubt that the small HOMO−LUMO gap contributed to the significantly reduced excitation energy. The small HOMO−LUMO gap may also add difficulty to TDDFT approaches in locating the structure of the $\pi \rightarrow \pi^*$ adiabatic excited state.

Among all TDDFT methods, the M052X functional was peculiar for having the greatest energy gaps between the HOMO and the LUMO (Figure 3). Noticing the big HOMO−LUMO gap, it is acceptable that M052X predicted slightly higher vertical excitation energies than the other functionals. Surprisingly, the adiabatic excitation energy from M052X was the lowest among all TDDFT functionals (Figure 2). We may trace this anomaly back to TDDFT methods. According to the response theory, excitation energy, ω, and corresponding vectors, $\mathbf{X}$ and $\mathbf{Y}$, were generally obtained by solving the following non-Hermitian eigenvalue equation.[29−31]

$$\begin{pmatrix} \mathbf{A} & \mathbf{B} \\ \mathbf{B} & \mathbf{A} \end{pmatrix} \begin{pmatrix} \mathbf{X} \\ \mathbf{Y} \end{pmatrix} = \omega \begin{pmatrix} \mathbf{1} & \mathbf{0} \\ \mathbf{0} & -\mathbf{1} \end{pmatrix} \begin{pmatrix} \mathbf{X} \\ \mathbf{Y} \end{pmatrix} \quad (2)$$

Therefore, we typically have both excitation from occupied Kohn−Sham MOs to virtual Kohn−Sham MOs (particle−hole) and excitation from virtual Kohn−Sham MOs to occupied Kohn−Sham MOs (hole−particle). The hole−particle components are also called de-excitation, which was negligible for the vertical excited states but appeared to be significant in all adiabatic excited states. The components of $\pi \rightarrow \pi^*$ excitation with the M052X functional had an important contribution of

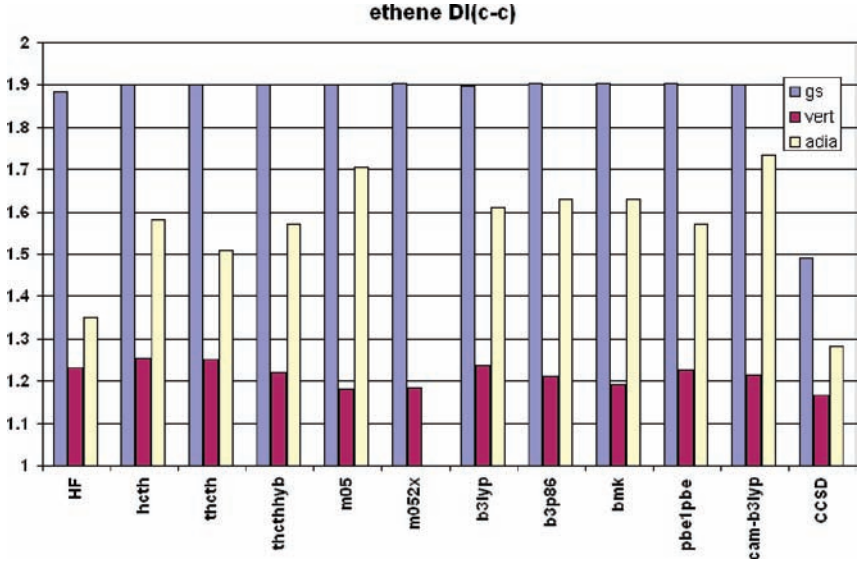

Figure 4. Calculated delocalization indices (DIs) for the ground state (gs), vertical excited state (vert), and adiabatic excited state (adia) of ethene. (Methods for ground states are HF, DFT, and CCSD, and the corresponding methods for excited states are CIS, TDDFT, and EOM-CCSD).

LUMO → HOMO de-excitation. The magnitude of the LUMO → HOMO coefficient was 1.732, whereas that of HOMO → LUMO was 1.839. The magnitude of the de-excitation coefficients for other functionals was approximately 0.5, which was about half of that of excitation coefficients (HOMO → LUMO).

In conclusion, DFT methods generally change the energies of Kohn−Sham MOs to treat systems at a more accurate stage than HF for the ground state. In the meantime, the energy increases of HOMO and energy decreases of LUMO typically result in too low excitation energy for the $\pi \rightarrow \pi^*$ excited state of ethene.

2.3. Delocalization Index Analyses. Electron density provides a common place to compare different methods via the density difference plots. Once electron density is derived, a molecule can be separated into QT-AIM atomic basins.[11] In this context, the DIs can be calculated by eq 1, which has been extended to study correlation effects in both ground and excited states.[12−17] We plotted C−C DIs in Figure 4 (cf. Table S1d in the Supporting Information for the exact values with both 6-311++G** and aug-cc-pVTZ basis sets) to compare the DFT methods with wave function methods for both ground and excited states.

The behavior of DIs (Figure 4) confirmed the observation that the DFT DIs for the ground states were normally close to or even bigger than HF DIs (blue bars),[10,13,18] whereas CCSD DIs were noticeably smaller than HF DIs. The increase in TDDFT DIs was particularly significant for the adiabatic excited states (yellow bars). For the vertical excited states, DIs were small for all three types of methods. Again, CCSD DI was smaller than CIS DI. DFT DIs roughly fall in between CIS DI and CCSD DI, and some DFT DIs could be slightly bigger than CIS DI. These above DI behaviors were explained by the occupation number of MOs, as explained below.

For the ground state, some virtual MOs of correlated wavefuntion files (such as CCSD, etc.) are occupied by a small amount of electrons. Those occupations mimic the contribution of other configurations in the conventional correlated methods. The occupation of virtual MOs explained the significant decrease in DIs for correlated methods. All virtual Kohn−Sham MOs of DFT wave function files for the ground states were empty because the current implementation of DFT adopts an HF-like single determinant. Therefore, the calculated DIs from DFT and HF wave function files were similar.

The occupation of virtual MOs also explains the DI trends for both the vertical and adiabatic excited states. As a general rule, smaller occupation numbers of virtual MOs would lead to a small decrease in DIs. For the vertical excited states, we had roughly one electron on each of the π and π^* MOs for all three types of methods; therefore, all CIS, TDDFT, and EOM-CCSD wave function files produced small DIs, which were in turn similar to one another. For the twisted adiabatic excited states, the significantly large DIs of TDDFT again were related to the occupation numbers of virtual MOs (mainly π^* MO). The occupation numbers of the ninth Kohn−Sham natural MOs (LUMO) in TDDFT wave function files were very small (0.002 to 0.168), whereas CIS still had roughly one electron in π^* MOs. The small LUMO occupation numbers for DFT methods were understandable considering the significant de-excitation from LUMO to HOMO. In the EOM-CCSD wave function files, aside from the doubly occupied inner MOs, electrons were scattered among a number of MOs (HOMO 1.11e, LUMO 0.86e, HOMO-1 through HOMO-5 each have 1.97 to 1.95e, and LUMO+1 through LUMO+5 each have 0.020 to 0.024e).

The DI was 1.5034 at the CCSD/aug-cc-pVTZ level and roughly 1.9 at DFT/aug-cc-pVTZ levels for the ground state of ethene (Table S1d in the Supporting Information). The DIs describe electron pair density or sharing magnitude, and DIs obtained with correlated wave function files are good approximations to those obtained from exact correlated treatment.[14a,16,17] If we focus only on first-order density, can we derive a bond order close to two based on electron density from the CCSD wave function file? The C−C bond order can be approximated by the equation of $b = (n - n^*)/2$, where n and n^* are occupation numbers of bonding and antibonding MOs, respectively. Regarding CCSD wave function files, the HOMO (π) and LUMO (π^*) have 1.915e and 0.064e, respectively. Additionally, MO6 (σ) and MO11 (σ^*) have 1.957e and 0.022e, respectively. Therefore, the bond order should be $(1.957 + 1.915 - 0.064 - 0.022)/2 = 1.893$. The value of 1.893 is close to 2, the ideal number for a covalent double bond. This relationship can be visualized by electron density difference plots (Figure 5). We subtracted the electron density of the HOMO (π) in the HF wave function file from the electron density of the HOMO (π) and LUMO (π^*) in the CCSD wave function file, and the electron density difference plots demonstrated obvious $\pi \rightarrow \pi^*$ character. Only taking the HOMOs of B3LYP and HF, we found

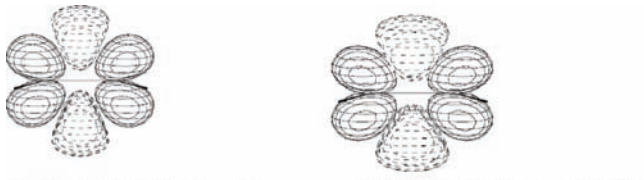

Figure 5. Density difference from specific MOs for the ground state of ethene (0.001 au contour, dotted line indicating density depletion, and solid line indicating density increasing).

a strikingly similar electron density difference plot. In summary, although DIs were much smaller for CCSD wave function files than for DFT wave function files, DFT methods and CCSD methods had similar electron density distributions. Because DFT methods included π^* character in π MOs, Kohn−Sham HOMOs of DFT methods had higher MO energy than HF HOMOs (Figure 3). Therefore, the significant changes in pair density might not also induce dramatic changes in density, suggesting that electron density itself may not be sensitive enough to account for multiple reference character.

3. Discussion

The adiabatic $\pi \rightarrow \pi^*$ excited state had not been previously carefully studied by TDDFT methods. Van Caillie and Amos implemented the gradient of TDDFT methods and tested only the lowest excited states of ethene and formaldehyde, and the lowest excited state of ethene with a small dihedral angle (33.4° at TD-LDA/6-311(2+,+)G** level) was the $\pi \rightarrow$ 3s excited state.[19] Furche and Ahlrich also implemented the gradient for TDDFT methods and investigated excited-state properties recently, but ethene was not included in their test set of small molecules.[32] However, the considerable underestimation of excitation energies by TDDFT was common for the charge transfer (CT) excited states because of the spurious self-interaction.[33−35] A special example was ethene dimer. Hieringer and Görling proved that the underestimation of excitation energies came from the imperfect TDDFT exchange-correlation kernel,[36] whereas Dreuw and Head-Gordon treated this special case as CT having exact degeneracy.[37] In the case of the adiabatic $\pi \rightarrow \pi^*$ excited state, the ideal structure should have a dihedral angle of 90°; therefore, π and π^* MOs would be exactly degenerate. The closer the dihedral angle approaches 90°, the worse the TDDFT excitation energies will be. This was confirmed by Figure 2. Although the adiabatic $\pi \rightarrow \pi^*$ excited state is a special case of CT excited states, it is normally classified to be of multiple-configuration characteristics.

The MO properties were helpful for interpreting results, and both occupied and virtual MOs needed to be considered in the study of excited states. According to the adiabatic approximation of TDDFT methods, the unknown time-dependent exchange-correlation potential of the excited state was approximated by the time-independent exchange-correlation potential of the ground state.[4,31] Within HF theory, the Koopman theorem indicated that −HOMO and −LUMO were good approximations for ionization potential (IP) and electron affinity (AP), respectively. The former was evaluated with the N electron system, and the latter was formally evaluated with the N + 1 system. Within the DFT framework, both −HOMO and −LUMO were estimated with the same N electron system; therefore, the HOMO energy was still related to the IP, but the −LUMO energy was usually too low, resulting in lower excitation energies.[35] The energies of −HOMO could be used to estimate the accuracy of TDDFT methods[38] and to design new functionals.[39] We classified all 24 DFT functionals (excluding LSDA) into three categories: pure GGA functionals (BLYP, OLYP, BP86, PBEPBE, HCTH), pure τ functionals (THCTH, BB95, VSXC, TPSSTPSS), and hybrid functionals (M05, M052X, O3LYP, B3LYP, B3P86, PBE1PBE, B1B95, THCTH-HYB, TPSSH, BMK, BHandH, BHandHHYB, HSE2PBE, HSE1PBE, CAM-B3LYP). As a general rule, pure functionals tended to introduce small HOMO−LUMO gaps, and hybrid functionals tended to give large HOMO−LUMO gaps because of their HF-exchange component. Therefore, the hybrid functionals normally predict excitation energies better than the pure functionals. The HOMO energies increased and LUMO energies decreased so dramatically at the same time (Figure 3) that the improvement with hybrid functionals was negligible for the $\pi \rightarrow \pi^*$ adiabatic excited states of ethene (Figure 2). For the vertical and adiabatic n_y-π^* excited state of H_2CO, HOMO energies markedly increased but LUMO energies only slightly decreased with DFT methods (Figure S1 in the Supporting Information) and thus the performance of hybrid functionals was obviously better (Figure S1a in the Supporting Information).

Because excited states usually involve more than two MOs and MOs normally span over the entire molecule, density analyses are necessary to characterize excited states. The density analyses were especially helpful in interpreting the results from the conventional correlated methods because the treatment of electron correlation needed to manipulate all MOs. Besides the density difference analyses, we can further perform pair density analyses (DI) in the QT-AIM framework[11] or undertake electron localization function (ELF)[40] analyses. Our detailed studies on DIs by the means of TDDFT (and DFT) indicated that further investigations were necessary for such analyses with TDDFT and DFT methods. Scalmani et al. recently included solvent effects during the implementation of the TDDFT gradient.[20] Therefore, solvent effects could also be included for both TDDFT optimization and TDDFT density analyses.

4. Conclusions

The detailed analyses of the MO properties for the ground state and the $\pi \rightarrow \pi^*$ excited state of ethene explained several aspects of the DFT and TDDFT methods: (1) The DFT methods included electron correlation effects by directly changing the electron density distributions among occupied MOs; the changes in electron density distribution were related to the energy increases for occupied MOs. (2) The correlation effects of DFT methods increased occupied MO energies and reduced virtual MO energies, contributing to the significant underestimation of excitation energies of ethene by TDDFT methods. (3) The apparent DI differences between DFT methods and conventional correlated methods were explained by the different MO occupation numbers. (4) For the $\pi \rightarrow \pi^*$ adiabatic excited states of ethene, the significant underestimation of the excitation energy can be attributed to the exact degeneracy of HOMO and LUMO, a special case of CT excited states.

5. Calculations

Both CIS and TDDFT (DFT) calculations were done with a development version of GAUSSIAN;[41] CASGEN[42] was used to make the electron density difference plots, and we employed AIMALL[43] or AIMPAC[44] to obtain the AOM. The DIs were obtained with LIDICALC.[45]

Supporting Information Available: Optimized C═C bond lengths of $\pi \rightarrow \pi^*$ excited states for ethene, the excitation energies of $\pi \rightarrow \pi^*$ excited states for ethene, FMO energies

for ethene, calculated DIs for the C=C bond with both 6-311++G** and aug-cc-pVTZ basis sets, and results for H_2CO. This material is available free of charge via the Internet at http://pubs.acs.org.

References and Notes

(1) Hohenberg, P.; Kohn, W. *Phys. Rev.* **1964**, *136*, B864.

(2) Kohn, W.; Sham, L. J. *Phys. Rev.* **1965**, *140*, A1133.

(3) Piela, L. *Ideas of Quantum Chemistry*; Elsevier: Amsterdam, 2007; pp 567−614.

(4) Koch, W.; Holthausen, M. C. *A Chemist's Guide to Density Functional Theory*; Wiley-VCH: Weinheim, Germany, 2000.

(5) Parr, R. G. *Annu. Rev. Phys. Chem.* **1983**, *34*, 631.

(6) Parr, R. G.; Yang, W. *Annu. Rev. Phys. Chem.* **1995**, *46*, 701.

(7) Parr, R. G.; Yang, W. *Density-Functional Theory of Atoms and Molecules*; Oxford University Press: Oxford, U.K., 1989.

(8) Scuseria, G. E.; Staroverov, V. N. In *Theory and Applications of Computational Chemistry: The First Forty Years*; Dykstra, C. E., Frenking, G., Kim, K. S., Scuseria, G. E., Eds.; Elsevier: Amsterdam, 2005; pp 669−724.

(9) Nakano, H.; Nakajima, T.; Tsuneda, T.; Hirao, K. In *Theory and Applications of Computational Chemistry: The First Forty Years*; Dykstra, C. E., Frenking, G., Kim, K. S., Scuseria, G. E., Eds.; Elsevier: Amsterdam, 2005, pp 507−580.

(10) (a) de Proft, F.; Sablon, N.; Tozer, D. J.; Geerlings, P. *Faraday Discuss.* **2007**, *135*, 151. (b) Ayers, P. W. *Faraday Discuss.* **2007**, *135*, 161. (c) Chandra, A. K.; Nguyen, M. T. *Faraday Discuss.* **2007**, *135*, 191. (d) Glukhov, I. V.; Lyssenko, K. A.; Korlyukov, A. A.; Antipin, Y. M. *Faraday Discuss.* **2007**, *135*, 203. (e) Garcia, P.; Dahaoui, S.; Katan, C.; Souhassou, M.; Lecomte, C. *Faraday Discuss.* **2007**, *135*, 217. (f) Bader, R. F. W.; et al. *Faraday Discuss.* **2007**, *135*, 237.

(11) Bader, R. F. W. *Atoms in Molecules: A Quantum Theory*; Clarendon Press: Oxford, U.K., 1990.

(12) (a) Bader, R. F. W.; Stephens, M. E. *J. Am. Chem. Soc.* **1975**, *97*, 7391. (b) Bader, R. F. W.; Streitwieser, A.; Neuhaus, A.; Laidig, K. E.; Speers, P. *J. Am. Chem. Soc.* **1996**, *118*, 4959.

(13) Fradera, X.; Austen, M. A.; Bader, R. F. W. *J. Phys. Chem. A* **1999**, *103*, 304.

(14) (a) Matito, E.; Sola, M.; Salvador, P.; Duran, M. *Faraday Discuss* **2007**, *135*, 325–367. (b) Poater, J.; Sola, M.; Duran, M.; Fradera, X. *Theor. Chem. Acc.* **2002**, *107*, 362. (c) Fradera, X.; Poater, J.; Simon, S.; Duran, M.; Sola, M. *Theor. Chem. Acc.* **2002**, *108*, 214.

(15) (a) Fulton, R. L. *J. Phys. Chem.* **1993**, *97*, 7516. (b) Fulton, R. L.; Mixon, S. T. *J. Phys. Chem.* **1993**, *97*, 7510. (c) Fulton, R. L.; Mixon, S. T. *J. Phys. Chem.* **1995**, *97*, 7510. (d) Fulton, R. L. *J. Phys. Chem. A* **2006**, *110*, 12191.

(16) (a) Wang, Y.-G.; Werstiuk, N. H. *J. Comput. Chem.* **2003**, *24*, 379. (b) Wang, Y.-G.; Matta, C. F.; Werstiuk, N. H. *J. Comput. Chem.* **2003**, *24*, 1720. (c) Wang, Y.-G.; Wiberg, K. B.; Werstiuk, N. H. *J. Phys. Chem. A.* **2007**, *111*, 3592.

(17) (a) Buijse, M. A.; Baerends, E. *Mol. Phys.* **2002**, *100*, 401. (b) Muller, A. M. K. *Phys. Lett.* **1984**, *105*, 446. (c) Goedecker, S.; Umrigar, C. J. *Phys. Rev. Lett.* **1998**, *81*, 866. (d) Holas, A. *Phys. Rev.* **1999**, *59*, 3454. (e) Cioslowski, J.; Pernal, K. *J. Chem. Phys.* **1999**, *111*, 3396.

(18) Kar, T.; Angyan, J. G.; Sannigrahi, A. B. *J. Phys. Chem. A* **2000**, *104*, 9953.

(19) (a) Van Caillie, C.; Amos, R. D. *Chem. Phys. Lett.* **2000**, *317*, 159. (b) Van Caillie, C.; Amos, R. D. *Chem. Phys. Lett.* **1999**, *308*, 249.

(20) Scalmani, G.; Frisch, M. J.; Mennucci, B.; Tomasi, J.; Cammi, R.; Barone, V. *J. Chem. Phys.* **2006**, *124*, 094107.

(21) Foo, P. D.; Innes, K. K. *J. Chem. Phys.* **1974**, *60*, 4582.

(22) (a) Ben-Nun, M.; Martinez, T. *J. Chem. Phys.* **2000**, *259*, 237. (b) Barbatti, M.; Paier, J.; Lischka, H. *J. Chem. Phys.* **2004**, *121*, 11614.

(23) (a) Lindh, R.; Roos, B. O. *Int. J. Quantum Chem.* **1989**, *35*, 813. (b) A survey and revisited study about this $^1B_{1u}V$ state is referred to in the paper by Müller: Müller, T.; Dallos, M.; Lischka, H. *J. Chem. Phys.* **1999**, *110*, 7176. and references therein.

(24) (a) Foresman, J. B.; Schlegel, H. B. In *Recent Experimental and Computational Advances in Molecular Spectroscopy*, Fausto, R., Ed.; Kluwer Academic Publishers: Dordrecht, The Netherlands, 1993, pp 11−26. (b) A review on the importance of multiconfiguration methods can be found in: Serrano-Andres, L.; Merchan, M. *THEOCHEM* **2005**, *729*, 99.

(25) Wiberg, K. B.; Hadad, C. M.; Foresman, J. B.; Chupka, W. A. *J. Phys. Chem.* **1992**, *96*, 10756.

(26) Wiberg, K. B.; Wang, Y.-G.; de Oliveira, A. E.; Perera, A.; Vaccaro, P. H. *J. Phys. Chem. A* **2005**, *10*, 9–466.

(27) (a) Goldstein, E.; Beno, B.; Houk, K. N. *J. Am. Chem. Soc.* **1996**, *118*, 6036. (b) Houk, K. N.; Beno, B. R.; Nendel, M.; Black, K.; Yoo, H. Y.; Wilsey, S.; Lee, J. K. *THEOCHEM* **1997**, *398*, 169. (c) Hrovat, D. A.; Beno, B. R.; Lange, H.; Yoo, H. Y.; Houk, K. N.; Borden, W. T. *J. Am. Chem. Soc.* **2000**, *122*, 7456.

(28) Chiba, M.; Tsuneda, T.; Hirao, K. *J. Chem. Phys.* **2006**, *124*, 144106.

(29) Crawford, T. D. *Theor. Chem. Acc.* **2006**, *115*, 227.

(30) Stratmann, R. E.; Scuseria, G. E.; Frisch, M. J. *J. Chem. Phys.* **1998**, *109*, 8218.

(31) (a) Casida, M. E. In *Recent Developments and Applications in Density Functional Theory*; Seminario, J. M., Ed.; Elsevier: Amsterdam, 1996. (b) Casida, M. E. In *Recent Developments and Applications in Density Functional Methods, Part I*; Chong, D. P., Ed.; World Scientific: Singapore, 1995.

(32) Furche, F.; Ahlrichs, R. A. *J. Chem. Phys.* **2002**, *117*, 7433.

(33) Schirmer, J.; Dreuw, A. *Phys. Rev. A* **2007**, *75*, 022513.

(34) Dreuw, A.; Head-Gordon, M. *Chem. Rev.* **2005**, *105*, 4009.

(35) (a) Dreuw, A.; Head-Gordon, M. *J. Am. Chem. Soc.* **2004**, *126*, 4007. (b) Dreuw, A.; Weisman, J. L.; Head-Gordon, M. *J. Chem. Phys.* **2003**, *119*, 2043. (c) Casida, M. E.; Gutierrez, F.; Guan, J.; Gadea, F.-X.; Salahub, D. R.; Daudey, J.-P. *J. Chem. Phys.* **2000**, *113*, 7062.

(36) Hieringer, W.; Gorling, A. *Chem. Phys. Lett.* **2006**, *419*, 557.

(37) Dreuw, A.; Head-Gordon, M. *Chem. Phys. Lett.* **2006**, *426*, 231.

(38) (a) Casida, M. E.; Jamorski, C.; Casida, K. C.; Salahub, D. R. *J. Chem. Phys.* **1998**, *108*, 4439. (b) Ciofini, I.; Adamo, C. *J. Phys. Chem. A* **2007**, *111*, 5549. (c) Rohr, D. R.; Gritsenko, O. V.; Baerends, E. J. *THEOCHEM* **2006**, *762*, 193.

(39) Tozer, D. J.; Handy, N. C. *J. Chem. Phys.* **1998**, *109*, 10180.

(40) (a) Poater, J.; Duran, M.; Sola, M.; Silvi, B. *Chem Rew.* **2005**, *105*, 3911–3947. (b) Becke, A. D.; Edgecombe, K. E. *J. Chem. Phys.* **1990**, *92*, 5397. (c) Savin, A.; Nesper, R.; Wengert, S.; Fassler, T. F. *Angew. Chem., Int. Ed.* **1997**, *36*, 1808.

(41) Frisch, M. J.; Trucks, G. W.; Schlegel, H. B.; Scuseria, G. E.; Robb, M. A.; Cheeseman, J. R. ; Montgomery, J. A., Jr.; Vreven, T.; Kundin, K. N.; Burant, J. C.; Millam, J. M.; Iyengar, S. S.; Tomasi, J.; Barone, V.; Mennucci, B.; Cossi, M.; Scalmani, G.; Rega, N.; Petersson, G. A.; Nakatsuji, H.; Hada, M.; Ehara, M.; Toyota, K.; Fukuda, R.; Hasegawa, J.; Ishida, M.; Nakajima, T.; Honda, Y.; Kitao, O.; Nakai, H.; Klene, M.; Li, X.; Knox, J. E.; Hratchian, H. P.; Cross, J. B.; Adamo, C.; Jaramillo, J.; Gomperts, R; Stratmann, R. E.; Yazyev, O.; Austin, A. J.; Cammi, R.; Pomelli, C.; Ochterski, J. W.; Ayala, P. Y.; Morokuma, K.; Voth, G. A.; Salvador, P.; Dannenberg, J. J.; Zakrzewski, V. G.; Dapprich, S.; Daniels, A. D.; Strain, M. C.; Farkas, O.; Malick, D. K.; Rabuck, A. D.; Raghavachari, K.; Foresman, J. B.; Ortis, J. V.; Cui, Q.; Baboul, A. G.; Clifford, S.; Cioslowski, J.; Stefanov, B. B.; Liu, G.; Liashenko, A.; Piskorz, P.; Komaromi, I.; Martin, R. L.; Fox, D. J.; Keith, T.; Al-Laham, M. A.; Peng, C. Y.; Nanayakkara, A.; Challacombe, M.; Gill, P. M. W.; Johnson, B.; Chen, W.; Wong, M. W.; Gonzalez, C.; Pople, J. A. *Gaussian*, version E.05; Gaussian, Inc.: Wallingford, CT, 2006.

(42) Rablen, P. R.; Hadad, C. M. *CASGEN*; Yale University: New Haven, CT, 1993.

(43) Keith, T. A. *AIMALL for SGI*; Yale University: New Haven, CT, 1996.

(44) Biegler-Konig, F. W.; Bader, R. F. W.; Tang, T.-H. *J. Comput. Chem.* **1982**, *3*, 317.

(45) Wang, Y.-G.; Werstiuk, N. H. *LIDICALC*, McMaster University: Hamilton, Ontario, 2002.

JP904007J